Mechanical stabilisation of bainite

P. H. Shipway and H. K. D. H. Bhadeshia

Compression experiments in which plastically deformed austenite is allowed to transform to bainite have revealed that bainite, like martensite, is susceptible to mechanical stabilisation. The overall transformation kinetics becomes slower and the maximum attainable fraction of bainite decreases in deformed austenite. This is because the motion of the transformation interface is hindered by the accumulated debris of dislocations in the austenite. The number density of nucleation sites is increased in deformed austenite, resulting in a more refined microstructure. Severe deformation eventually leads to a recovery in the maximum attainable fraction of bainite because of the corresponding increase in nucleation site density. *MST/3148*

 Manuscript received 25 August 1994; in final form 14 October 1994. *At the time the work was carried out the authors were in the Department of Materials Science and Metallurgy, University of Cambridge. Dr Shipway is now in the Department of Materials Engineering and Materials Design, University Park, Nottingham.*

Introduction

Displacive transformations involve the coordinated movement of atoms, and such movements cannot be sustained against strong defects such as grain boundaries. Thus, martensite plates, which form by a displacive mechanism, cannot cross grain boundaries. Less potent defects such as isolated dislocations hinder the progress of such transformations, but the defect, if isolated, can often be incorporated into the martensite lattice. However, it is well established[1–6] that the heavy deformation of austenite before its transformation hinders the growth of martensite, leading to a smaller fraction of overall transformation even though its heterogeneous nucleation rate is increased in correspondence with the larger defect density. Another way of visualising this mechanical stabilisation is in terms of the structure of the transformation interface. Displacive transformations are accomplished by the advance of glissile interfaces which can be rendered sessile by the accumulation of dislocation debris. Thus, whereas an appropriate stress can stimulate displacive transformation in the same way that it enables normal deformation,[7,8] mechanical stabilisation actually retards the decomposition of the austenite.

Most of the work carried out on mechanical stabilisation effects has involved steels, and focused on the martensite transformation. The growth of bainite also leads to an invariant plane strain shape deformation with a large shear component which is similar to that of martensite, implying a coordinated movement of the iron and substitutional solute atoms. It should therefore also be susceptible to mechanical stabilisation, but this has not been properly established. A recent review[9] has demonstrated that there is some evidence indicating mechanical stabilisation effects. Hot rolling experiments by Davenport[10] can be interpreted as showing that bainitic transformation is retarded in deformed austenite. More direct evidence comes from the work of Tsuzaki *et al.*[11] who found that although deformed austenite transformed faster, the net volume fraction of bainite that formed decreased when compared with undeformed austenite.

Huang *et al.*[12] showed that deformed austenite transforms to bainite at a higher temperature during continuous cooling and at a faster rate, as long as the cooling occurred sufficiently fast to suppress recovery of the austenite. Similar effects were reported by Smith and Siebert,[13,14] who observed increases in the bainite start temperatures of up to 100°C at fast cooling rates. Such phenomena have not been observed in the isothermal transformation experiments reported in the present study.

Maki[15] found that ausforming markedly increases the rate of transformation of upper bainite, with a smaller effect on the lower bainite reaction (the progress of which

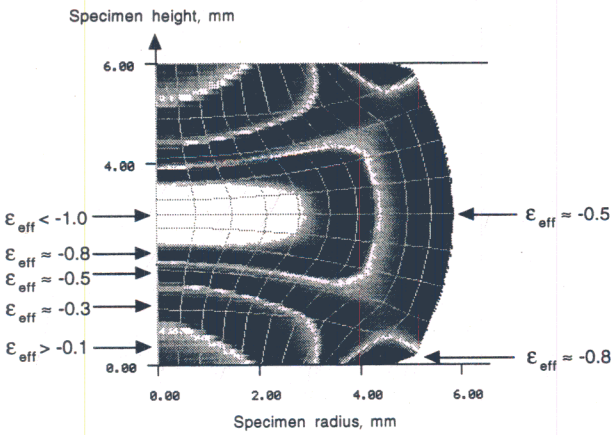

1 Finite element model calculation of strains in cylinder of initial height 12 mm and radius 4 mm compressed to final height of 6 mm with interfacial friction coefficient of 0·5 (half cylinder shown): values of strain contours are as indicated

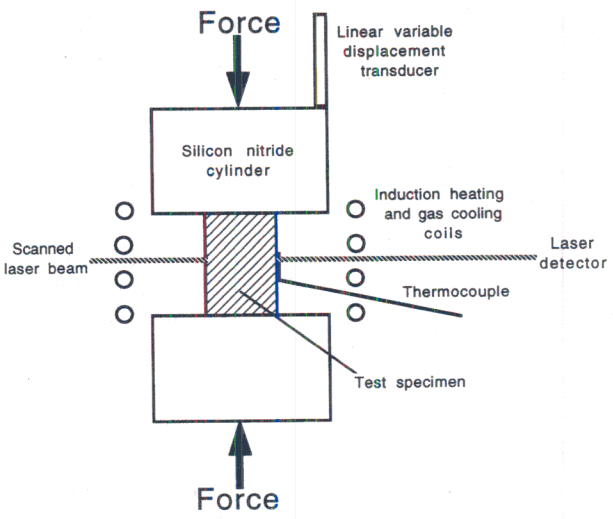

2 Schematic diagram of apparatus used for thermomechanical testing

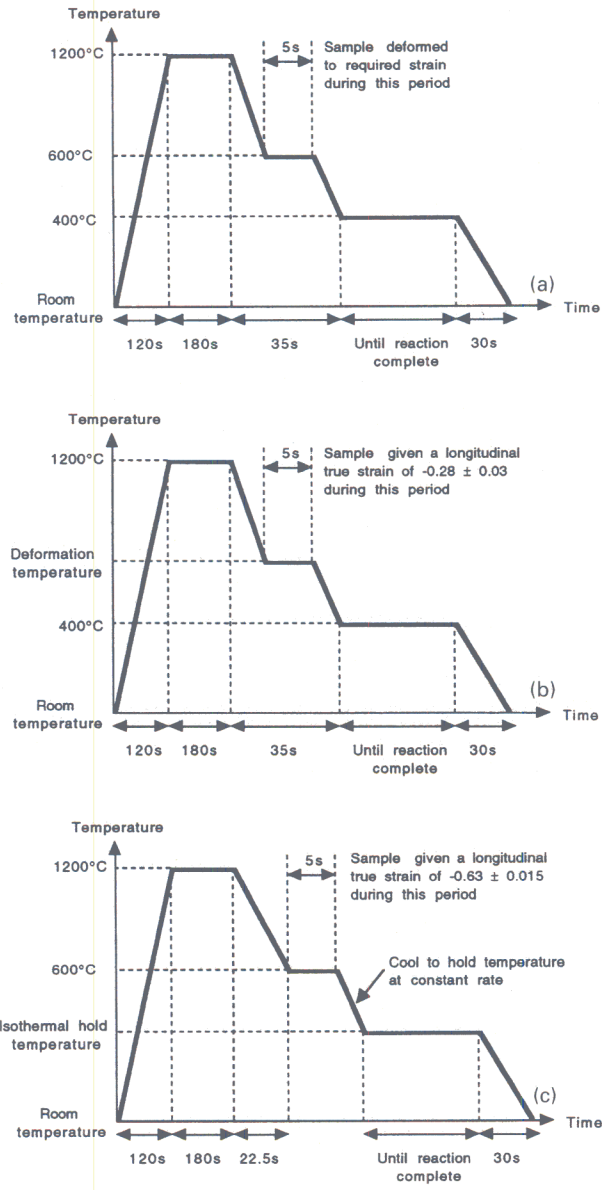

3 Thermal and mechanical cycles of test series used to examine effect of *a* total strain, *b* deformation temperature, and *c* transformation temperature

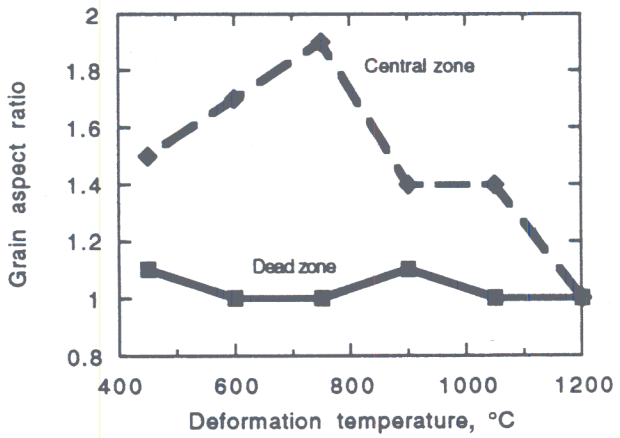

4 Prior austenite grain aspect ratio in dead zone and central region following deformation to true longitudinal strain of −0·28 as function of deformation temperature

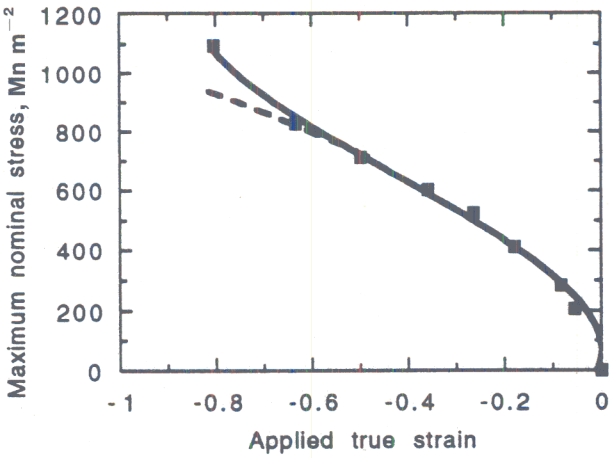

5 Maximum nominal applied stress as function of total applied longitudinal true strain for samples deformed at 600°C in 5 s

was eventually retarded). The plates of bainitic ferrite were thinner and contained a larger dislocation density when growing from deformed austenite. It was concluded that the bainite inherited the defect structure of the austenite. Edwards and Kennon[16] had previously reported the same observations and in addition, demonstrated nucleation of bainite from slip bands. Freiwillig *et al.*[17] also reported accelerated transformation to bainite from deformed austenite.

Other studies are more difficult to interpret. In the experiments of Bhattacharyya and Kehl,[18] the bainite was formed from deformed austenite, but under the influence of an applied stress; the latter can complicate the interpretation.[19] In microalloyed steels, strain induced precipitation of carbides, carbonitrides, or borides can influence the subsequent transformation of austenite.[20]

In summary, plastic deformation of austenite has been reported generally to accelerate the transformation to bainite, although the final quantity of bainite that forms may be reduced. This is consistent with the enhanced nucleation on defects combined with the retardation of growth by dislocation debris, i.e. mechanical stabilisation of the type familiar in literature concerning martensite.

In all instances the kinetics has been assessed using dilatometric or metallographic techniques which ignore the inevitable inhomogeneous nature of the deformation in the austenite. The purpose of the present work is to take advantage of this inhomogeneity in deformation to study the role of strain and transformation temperature on the extent of transformation. As discussed above, the published literature suggests that plastically deformed austenite should transform more rapidly to bainite. However, as is demonstrated below, the transformation may be accelerated or retarded depending on the level of plastic strain.

Table 1 Hardness of mixed microstructures produced from undeformed austenite

Isothermal transformation temperature, °C	Vickers hardness, HV0·5
500	754 ± 8
480	772 ± 6
440	750 ± 11
400	493 ± 10
360	456 ± 3
300	571 ± 7
260	633 ± 10
240	622 ± 3
Quenched	769 ± 6

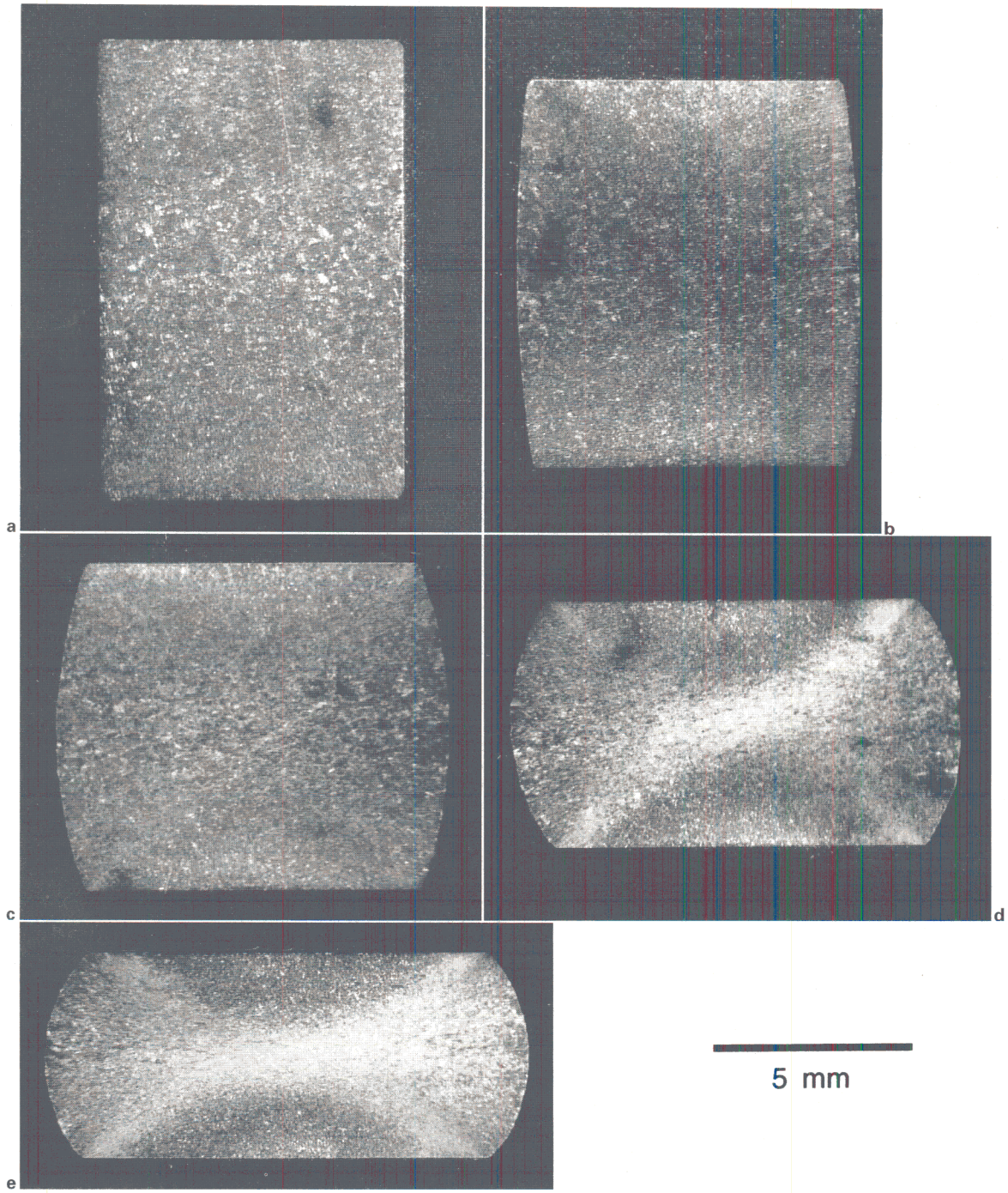

a 0·0; *b* −0·18; *c* −0·36; *d* −0·63; *e* −0·80

6 Macrographs of meridional planes of samples following thermomechanical cycle shown in Fig. 3*a* with various applied longitudinal true strains

Experimental method

TEST MATERIAL

The alloy used in the present work was 0·45C–2·08Si–2·69Mn–Fe (compositions in wt-% unless otherwise stated). The material was homogenised at 1250°C for 72 h in a pure argon atmosphere in a sealed quartz tube and then quenched in water to ensure uniform composition of the starting material. The alloy has sufficient hardenability to avoid high temperature transformations, and also transforms slowly to bainite, making isothermal experiments easier to perform.

Cylindrical specimens (8 × 12 mm in length) were machined for straining in uniaxial compression. Friction between the cylinder faces and the test machine platens is expected to cause barrelling of the cylinder; thus, the degree of strain in the sample will be a function of location, as shown by the finite element model (Deform – commercially available package) calculation in Fig. 1. The diagram is illustrative; the actual strains depend on flow stress, work hardening rate, strain rate sensitivity, and platen–workpiece friction coefficient. However, it shows the wide range of strains expected to occur in such a test. In this instance, the longitudinal true strain is −0·69, but there are regions close to the platen face where the effective strains are not

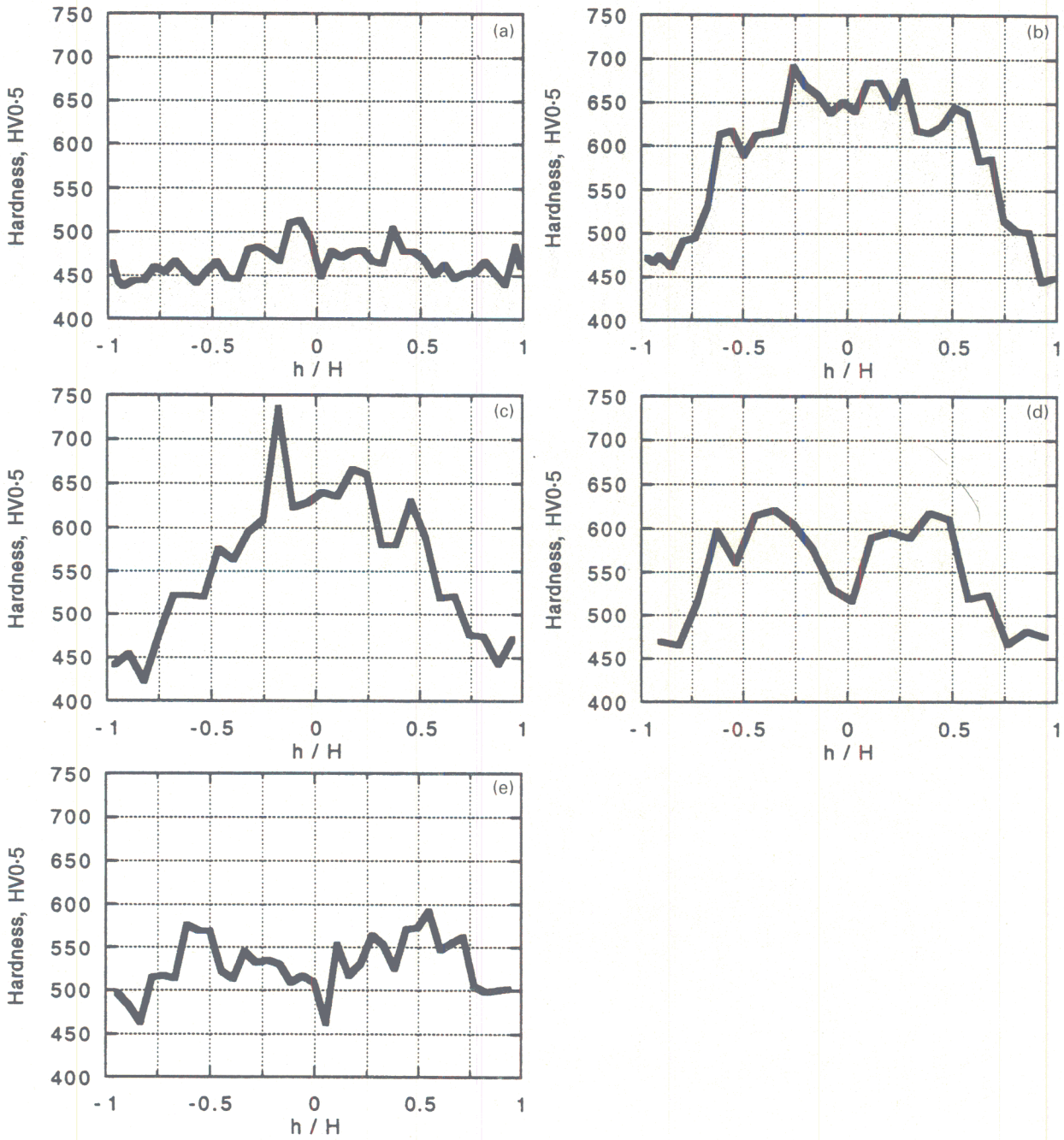

a 0·0; *b* −0·18; *c* −0·36; *d* −0·63; *e* −0·80

7 Hardness profiles along specimen axes of samples following thermomechanical cycle shown in Fig. 3*a* with various applied longitudinal true strains (*H* = cylinder half height, *h* = distance from centre of specimen)

much greater than −0·1 (the 'dead zone'), and regions in the centre where the effective strain is close to −1·0. The strain decreases along the axis of compression from the specimen centre to the platen face, and also decreases away from the centre towards the specimen edge in a direction normal to the compression axis. Such variations in strain should be reflected in microstructural changes within any given specimen; the extent of transformation can be monitored using microhardness measurements.

THERMOMECHANICAL TESTING

Thermomechanical treatments were carried out using an adapted Thermecmastor Z simulator which allowed control of the sample temperature, uniaxial load, and strain. Figure 2 shows a schematic diagram of the experimental arrangement. The sample was heated by induction in a high vacuum ($\sim 4 \times 10^{-2}$ Pa). A Pt/PtRh (type R) thermocouple was attached centrally to the sample surface; in another experiment, the measured temperature variation along the sample length was established to be less than ± 10 K. The sample was cooled at the desired rate using helium gas. Helium is used in preference to nitrogen in order to achieve higher cooling rates and more accurate control. Deformation was applied using a servohydraulic system, with either load or displacement control of the ram position. The system is capable of applying loads of up to 55 kN, the load being applied via silicon nitride cylinders. The sample temperature, load, time, and longitudinal

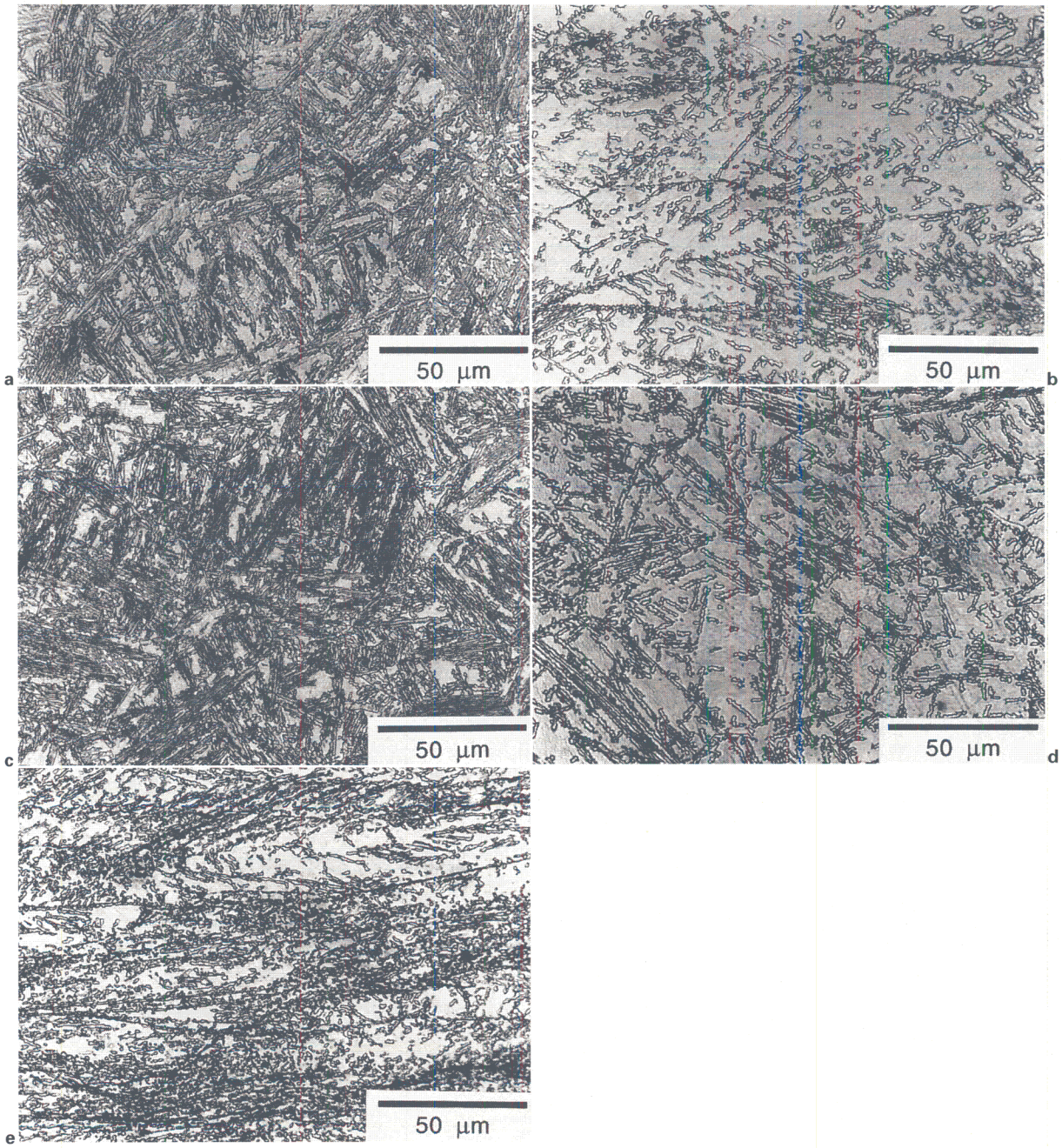

a dead zone, longitudinal true strain = −0·36; *b* central region, longitudinal true strain = −0·36; *c* dead zone, longitudinal true strain = −0·63; *d* between dead zone and central region, longitudinal true strain = −0·63; *e* central region, longitudinal true strain = −0·63

8 Optical microscopy (OM) images of bainite microstructures formed after thermomechanical treatment shown in Fig. 3*a*

displacements were measured concurrently. The strain was detected using a linear variable displacement transducer.

Three types of test were conducted. A set of samples was deformed to varying degrees at 600°C in the austenitic condition after treatment at 1200°C. The deformation was followed by isothermal transformation to bainite at 400°C. A second set of similarly austenitised samples was deformed at different temperatures to a constant longitudinal true strain of $-0{\cdot}28 \pm 0{\cdot}03$, followed by transformation to bainite at 400°C. A further series of samples was given a larger strain of $-0{\cdot}63 \pm 0{\cdot}015$ at 600°C, and then transformed to bainite at different temperatures. Figure 3 shows the three different treatments and time periods involved.

All deformations were achieved at constant velocity rather than constant strain rate, and were applied over a 5 s period regardless of the magnitude of the final strain. Following sample deformation, the position of the crosshead was switched to load control, and the growth of bainite occurred with an applied longitudinal compressive stress of ~ 1 MN m^{-2}, which is the minimum necessary to allow the longitudinal strain to be monitored throughout the transformation. Matsuzaki *et al.*[19] have shown that this compressive stress has a negligible effect on the bainite reaction. Note that in all cases, the isothermal transformation time was sufficient to allow the reaction to stop. Following the transformation, the sample was gas quenched to room temperature.

Optical metallography was conducted on meridional plane sections of the cylindrical samples. Microhardness tests were performed using a Leitz Miniload tester with a

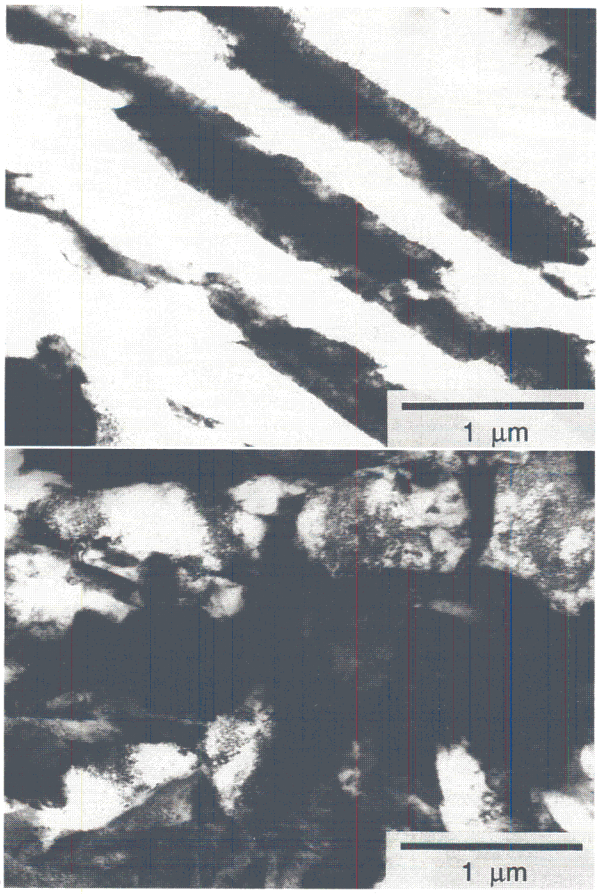

a dead zone; *b* deformed central region

9 Transmission electron microscopy (TEM) images of representative areas of sample deformed to longitudinal true strain of −0·63 in thermomechanical cycle shown in Fig 3*a*: white or lighter shaded areas are bainite, surrounded by darker martensite

Vickers pyramidal indenter and an indenting force of 0·5 kg. The load chosen was a compromise allowing indentations to be placed reasonably close together but also sampling a reasonable area of microstructure (the indentation diagonals were typically between 35 and 45 μm in length). Indentations were made at spacings of 300 μm along the compression axis of samples.

Following indentation, the samples were reground, polished, and etched with a 2% nital solution which preferentially etches bainite. Micrographs were obtained by optical microscopy (OM). Samples in the form of thin foils (prepared by electropolishing 100 μm thickness discs in 5% perchloric acid, 25% glycerol, 70% methanol solution at about −10°C, and with a polishing potential of ~60 V) were examined by transmission electron microscopy (TEM) using a Philips 400T microscope operating at 120 kV.

To assess the effect of deformation on grain size and shape, samples were quenched immediately following deformation at high temperatures. Samples were sectioned along the meridional plane and etched (using a solution of 2 g picric acid and 0·5 g copper(II) chloride in 100 ml of water, and with 2 ml wetting agent) to define clearly the prior austenite grain boundaries. Grain sizes were determined using the method of linear intercepts along randomly oriented lines, using more than 50 intercepts/measurement. Linear intercepts parallel and perpendicular to the specimen axis were also obtained and used to compute the grain aspect ratio. These experiments also confirmed that no bainite was formed during deformation of the sample in any of the tests.

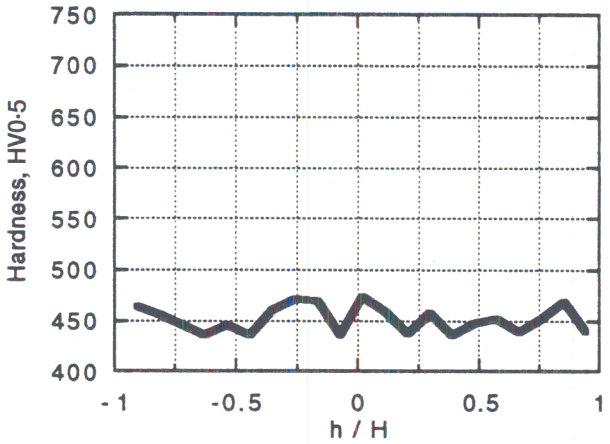

10 Hardness profile along axis of specimen following deformation to longitudinal true strain of −0·63 at 600°C, reheating to 1200°C for 180 s, and following thermal cycle shown in Fig. 3*a* with no further deformation (*H* = cylinder half height, *h* = distance from centre of specimen)

Results and discussion

HARDNESS OF HOMOGENEOUS SAMPLES

To assess the heterogeneous microstructures produced in the compression experiments, a number of experiments were conducted in which unstrained samples were transformed at different temperatures and their hardnesses measured, as given in Table 1. All of the heat treatments led to homogeneous microstructures; the hardness data represent the mean of 10 indentations in each case and are listed along with the standard error in the mean. The data show that the highest hardness occurs for the fully martensitic specimen as expected. All other microstructures are mixtures of bainitic ferrite and martensite. At first the hardness progressively decreases as the isothermal transformation temperature is reduced, since the maximum volume fraction of bainite that can form increases as the temperature decreases as a direct consequence of the incomplete reaction phenomenon.[9] The hardness starts to rise again as the isothermal transformation temperature is reduced below about 360°C. As will be seen below, this is partly due to refinement of the microstructure at lower temperatures. The refinement of individual platelets of bainitic ferrite also leads to a reduced overall degree of transformation as each nucleus grows into a smaller plate at low temperatures.

GRAIN SIZE AND SHAPE IN DEFORMED SAMPLES

The grain size in the dead zone of the samples deformed to a longitudinal true strain of approximately −0·28 was independent of deformation temperature in the range 450–1200°C, and the mean for each sample was within the range 44–66 μm. For samples deformed below 750°C, no recrystallisation was observed; deformation at 1200°C resulted in a fully recrystallised structure, at 1050°C in a partially recrystallised structure, and at 900°C in a small amount of recrystallisation around the grain boundaries. The mean grain sizes in the central regions of unrecrystallised specimens were larger than in the dead zones (due to the thermal gradient) and were in the range 70–110 μm. However, the mean grain sizes in the substantially recrystallised samples deformed at 1200 and 1050°C were 43 and 28 μm respectively.

Figure 4 shows the grain aspect ratio as a function of deformation temperature for longitudinal strains of

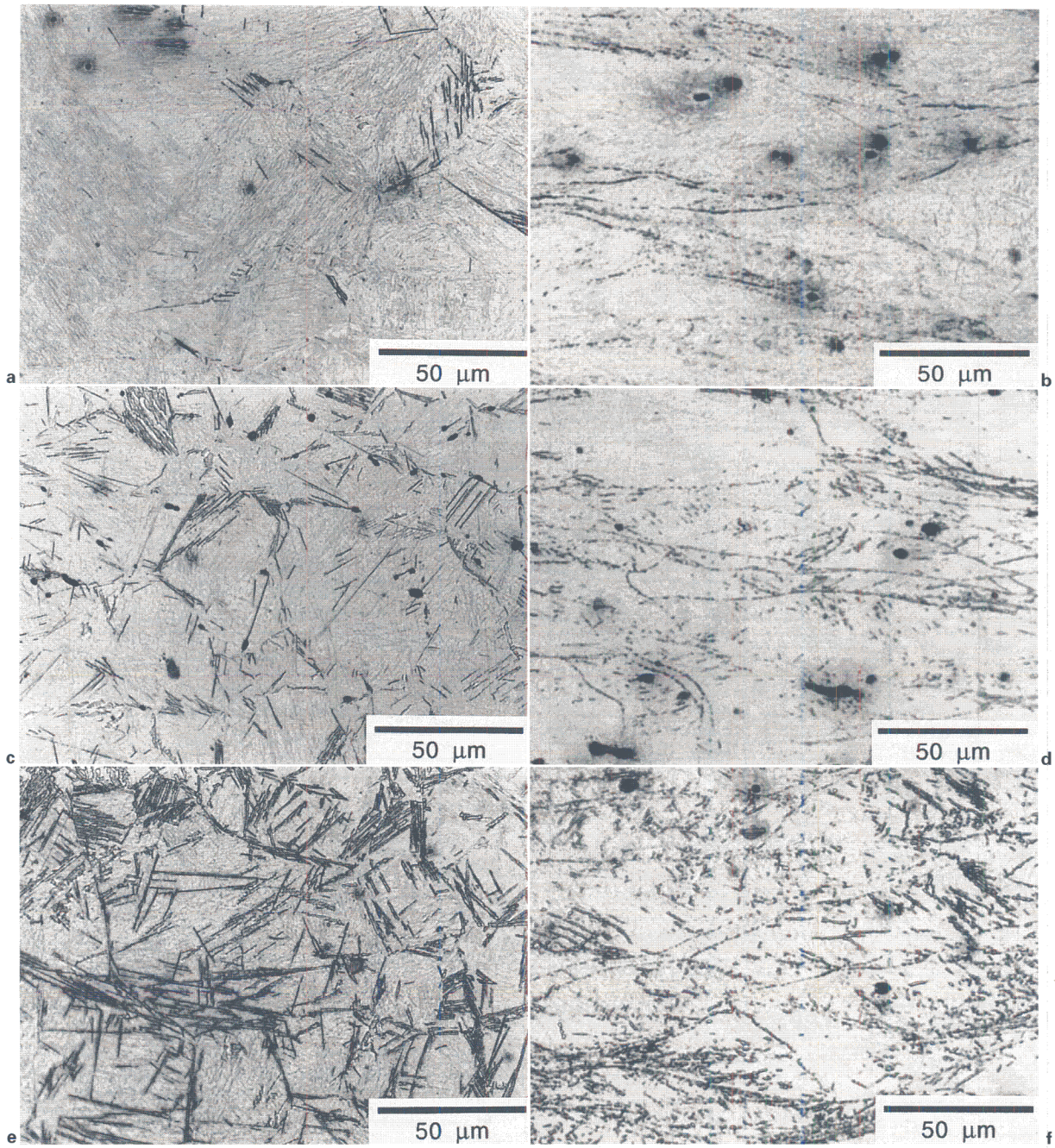

a dead zone, 100 s; *b* central zone, 100 s; *c* dead zone, 200 s; *d* central zone, 200 s; *e* dead zone, 500 s; *f* central zone, 500 s

11 Development of bainite in dead zone and central region of sample given longitudinal true strain of −0·63 (thermomechanical cycle shown in Fig. 3*a*) for different isothermal hold times (OM)

approximately −0·28 for both the central regions and dead zones. Deformation at the lower temperatures leads to grains with a high aspect ratio; this is reduced at high temperatures and is unity for deformation at 1200°C where full recrystallisation has occurred. A sample which was deformed to a longitudinal true strain of approximately −0·63 at 600°C showed no recrystallisation, and had a grain aspect ratio of 3·4 in the central region.

EFFECT OF TOTAL STRAIN

The engineering stress–true strain relationship for the deformation of austenite at 600°C, except at the largest compression, is approximately parabolic as might be expected from the usual work hardening models (Fig. 5). The rapid increase at the largest strains occurs as the dead zones at each end of the specimen begin to substantially interfere with each other.

Figure 6 shows optical macrographs of five samples with the austenite strained in the range 0 to −0·8 at 600°C before bainitic transformation at 400°C. The deformation is clearly not homogeneous; the main features are:

(i) the obvious dead zones at both ends of each sample (*cf.* Fig. 1)

(ii) the greater intensity of deformation in the core of the sample, extending in the shape of an X, and a lower degree of deformation than this, even at the sides of the samples

(iii) an increase in the gradients of deformation as the overall strain is increased.

The obvious gradient in strain along the sample axis provides an ideal opportunity to study the mechanical

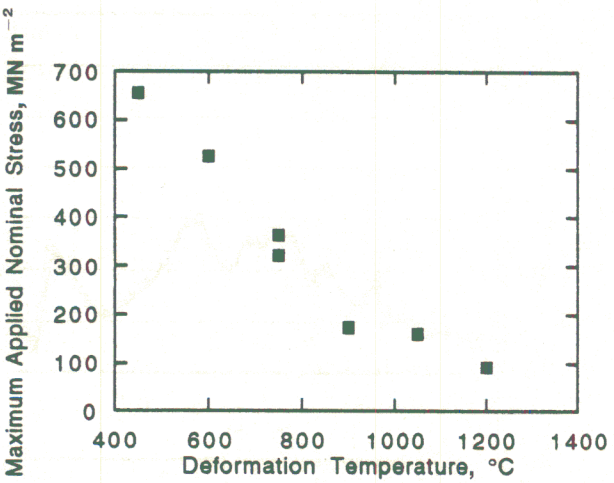

12 Maximum nominal applied stress as function of deformation temperature for samples deformed to longitudinal true strain of −0·28 in 5 s

stabilisation of bainite. The corresponding hardness traverses along the sample centerline are shown in Fig. 7 (a lower hardness at any transformation temperature is generally consistent with a greater degree of transformation to bainite). The sample transformed from unstrained austenite (Fig. 7*a*) has hardness values which are relatively uniform, with a slightly higher hardness at the sample centre, but in general consistent with the data given in Table 1 for transformation at 400°C. The slightly larger degree of transformation at the sample ends is attributed to lower temperatures in these regions owing to heat extraction via the silicon carbide platens.

Major changes occur in the microhardness profiles if the austenite is strained before transformation. At the low overall strains of −0·18 and −0·36 (Fig. 7*b* and *c*, respectively), the central regions contain very little bainite, with hardness levels in excess of 700 HV0·5, approaching that of a fully martensitic sample (*see* Table 1), whereas at the sample ends where the dead zones occur, the hardness data are consistent with the full permitted extent of reaction at 400°C. This is conclusive evidence for mechanical stabilisation in the central region of the sample where the strain is greatest. The hardness data are supported by optical microscopy (Fig. 8*a* and *b*) which shows clearly that there is a larger amount of bainite in the dead zone as opposed to in the sample core.

Another phenomenon is apparent from Fig. 7*d*, where the overall strain in the austenite is increased to −0·63. A significant minimum in hardness occurs in the central region. Thus, it has been demonstrated that a small amount of strain (in the region between the platen and the central region) mechanically stabilises the austenite, but that a larger degree of strain stimulates reaction. This is apparent in Fig. 8*c*–*e*. The deformation always hinders transformation, in the sense that the bainite is clearly more refined in the samples illustrated in Fig. 8*d* and *e*. Thus, once nucleated, the bainite is prevented from growing by the dislocation debris in the austenite, and the amount of transformation per plate of bainite is reduced. However, the nucleation rate is increased so that at a large enough value of strain, the sample is able to achieve an extent of transformation which is comparable with that in the undeformed regions. The microstructure shown in Fig. 8*e* is much more refined compared with that shown in Fig. 8*c*; this refinement was also evident from TEM (*see* Fig. 9), where it can be seen that the bainite plates are more irregular and smaller in length when formed from deformed austenite.

It is interesting to note that when bainite grows from undeformed austenite, the individual platelets are restricted in their growth by the plastic accommodation of the large IPS shape change.[9] The platelets therefore typically remain much smaller than the austenite grain size; their maximum length is about 10 μm. This plastic accommodation creates dislocation debris which leads to a loss of coherency at the transformation interface and consequently stops growth until a new platelet is nucleated. If the dislocation density of the austenite is increased by prior deformation, then the platelets are expected to be restricted at an earlier stage of growth, and this is indeed the case (Fig. 9). This effect can only be explained by a displacive mechanism of transformation.

To verify that dislocation debris was causing the observed effects on the development of the bainite microstructure, a sample was deformed at 600°C to a longitudinal true strain of −0·63, and then immediately reheated to 1200°C, held at this temperature for 180 s, and cooled to 400°C in the same manner as other samples in this series (*see* Fig. 3*a*) with no further deformation. The sample showed a homogeneous microstructure with no evidence of mechanical stabilisation of austenite. Figure 10 shows a hardness profile along the axis of the specimen which is clearly homogeneous (*cf.* Fig. 7*a* with no deformation, and Fig. 7*d* with a true strain of −0·63). The recovery and recrystallisation of this sample at high temperature has eliminated much of the dislocation debris and thus allowed normal growth of bainite.

Figure 11 shows the progress in the transformation of the −0·63 strained specimen in the dead zone and in the core. The experiments involved the quenching of partially transformed samples after a variety of transformation times. The incubation time is not affected by the deformation but the microstructure is clearly more refined at all stages in the deformed austenite.

EFFECT OF DEFORMATION TEMPERATURE

The experiments discussed above indicated that the hardness profiles showed maximum heterogeneity at strains between −0·18 and −0·36. Thus, the effect of deformation temperature was studied for an intermediate strain of −0·28. Figure 12 emphasises that the effect of raising the austenite deformation temperature is to make the deformation easier, so that mechanical stabilisation effects should diminish as the deformation temperature is raised. This is evident from the microhardness data shown in Fig. 13 and from the representative micrographs presented for the sample cores (Fig. 14).

Thus, the fraction of bainite formed in the central region of a sample at 400°C decreases as the sample deformation temperature decreases from 1200 to 600°C, and this is due to the fact that recovery can occur more readily at high temperatures.

There is a complicating feature concerning the austenite deformed at 450°C. The application of only 20 MN m^{-2} of compression stress has been reported[21] to induce bainite formation in this alloy at this temperature. It is possible that the application of >600 MN m^{-2} in the present experiment stimulated some transformation at the deformation temperature (450°C), which then enhanced subsequent transformation at 400°C. Thus, there appears to be a slightly higher quantity of bainite in the central region of samples deformed at 450°C compared with samples deformed at 600°C (*cf.* Fig. 14*f* with Fig. 14*e*).

EFFECT OF TRANSFORMATION TEMPERATURE

All samples discussed in the present work were deformed to a true strain of −0·63 ± 0·015 at 600°C before transformation to bainite at a variety of temperatures. This was the value of strain which led to the new observation that a

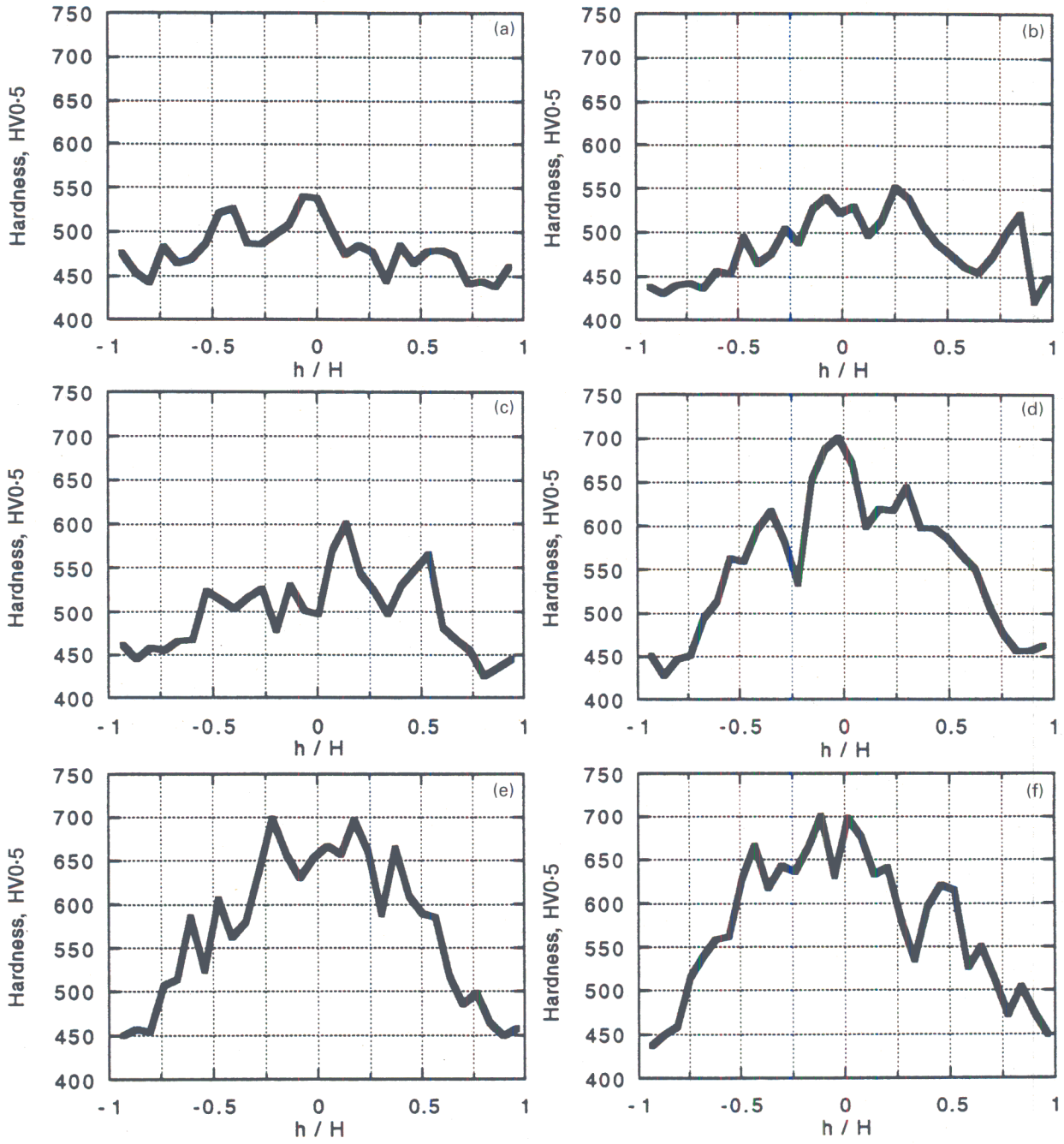

a 1200°C; *b* 1050°C; *c* 900°C; *d* 750°C; *e* 600°C; *f* 450°C

13 Hardness profiles along specimen axis of samples (after thermomechanical cycle shown in Fig. 3*b*) for various deformation temperatures (*H* = cylinder half height, *h* = distance from centre of specimen)

slight deformation stabilises austenite, but larger deformations cause a recovery in the volume fraction of bainite via an enhanced nucleation effect.

Figure 15 shows pairs of micrographs taken from the dead zone (*a*, *c*, *e*, *g*, *i*, *k*, *m*, *o*) and central, highly deformed regions (*b*, *d*, *f*, *h*, *j*, *l*, *n*, *p*). The isothermal transformation temperatures in Fig. 15 decrease from the pair *a*, *b* to the pair *o*, *p*, and corresponding microhardness profiles are shown in Fig. 16.

At 500°C a very small amount of bainite formed in the dead zone, but the central, more heavily deformed region began to transform to pearlite (Fig. 15*a* and *b*); the inset TEM micrograph of one of the dark bands seen in the optical micrograph confirms the presence of pearlite. Therefore, in this instance the central region has a lower hardness than the dead zone (Fig. 16*a*). Pearlite forms by the reconstructive transformation of austenite, a mechanism which involved the diffusion of all atoms. Such transformations are not hindered by defects such as dislocations, indeed, their nucleation can be enhanced so that reconstructive transformations are always accelerated by deformation. Similar results are obtained by transformation at 480°C, but the amount and size of the pearlitic regions is reduced because of the lower atomic mobility at this temperature (Fig. 15*c* and *d*). Consequently, the hardness in the central region increases relative to the 500°C sample. It is interesting that in both cases the formation of bainite has been suppressed in the central region, and that of pearlite accelerated, consistent with their displacive and reconstructive transformation mechanisms, respectively.

The microhardness data for the samples transformed at 440 and 400°C in Fig. 16 show similar behaviour to the

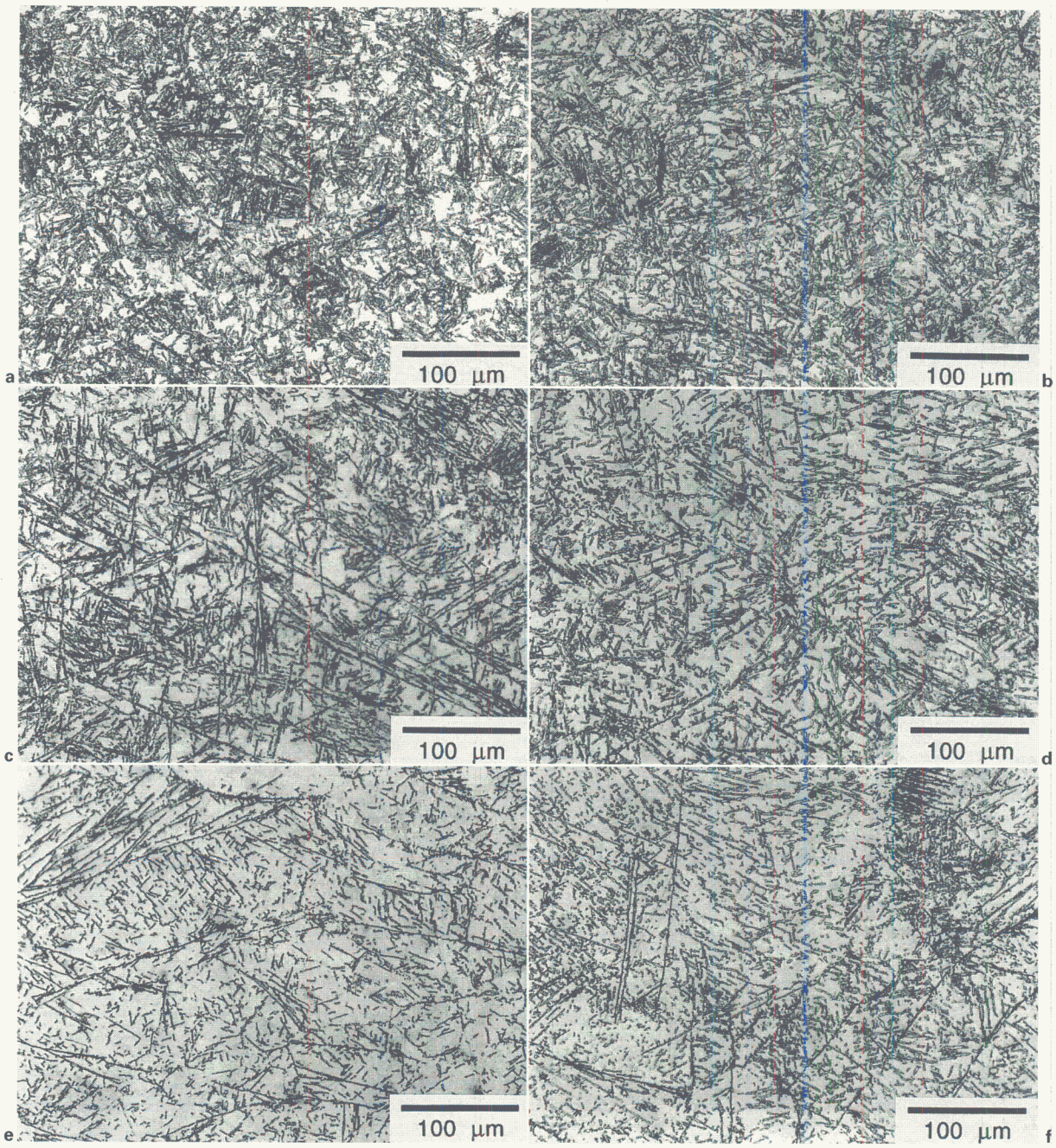

a 1200°C; *b* 1050°C; *c* 900°C; *d* 750°C; *e* 600°C; *f* 450°C

14 Bainite microstructures formed in central region (after thermomechanical treatment shown in Fig. 3*b*) at different deformation temperatures (OM)

results shown in Fig. 7 and require no further explanation. It is interesting, however, that the form of the hardness profile changes completely as the transformation temperature is reduced further. An increase in the chemical driving force with increasing undercooling below the bainite start temperature enables higher degrees of transformation to be achieved, so that the hardness profiles become more uniform and show lower values (Fig. 16*e* and *f*). This is confirmed by metallography as shown in Fig. 15*i*, *j*, *k*, and *l*. The effect of the larger chemical driving force is so pronounced that the hardness of the 300°C (Fig. 16*f*) sample is very similar at the core and the dead zone. The bainite is able to grow despite the dislocation debris present at these temperatures; the efficacy of the dislocations in preventing growth of bainite is reduced as the driving force for bainite growth increases.

The effect observed for transformation at 260 and 240°C (Figs. 15*m*, *n*, *o*, *p* and 16*g*, *h*) requires further comment. The overall hardness rises considerably. The sample transformed at 260°C shows some bainitic transformation in both the dead zone and in the core region (Fig. 15*m*, *n* respectively), and this was confirmed using TEM (Fig. 17). The optical metallography and TEM show a very pronounced refinement of the bainite plate thickness, from between 0·5 and 1·0 μm (Fig. 9*a*) to about 0·2 μm (Fig. 17*a*), which should lead to an increase in strength of about 260 MN m^{-2} (Ref. 22). This may explain some of the increase in hardness. However, the increase is dramatic, and it is also evident that the amount of bainite has decreased (Fig. 15*m*, *n*, *o*, *p*) in lowering the transformation temperature below 300°C. This occurs since each nucleus contributes less to the overall transformation as the bainite

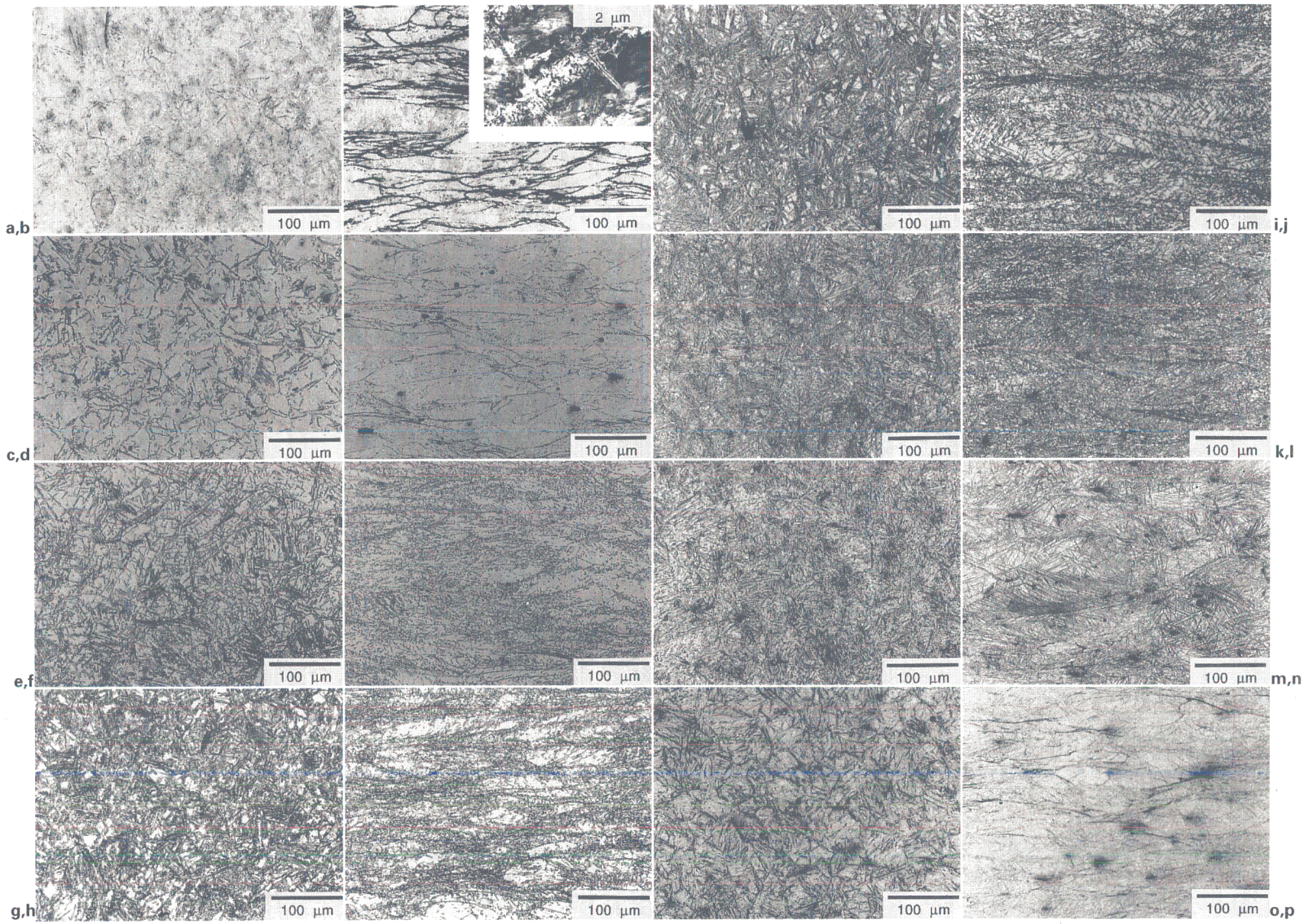

a dead zone, 500°C; *b* central region, 500°C; *c* dead zone, 480°C; *d* central region, 480°C; *e* dead zone, 440°C; *f* central region, 440°C; *g* dead zone, 400°C; *h* central region, 400°C; *i* dead zone, 360°C; *j* central region, 360°C; *k* dead zone, 300°C; *l* central region, 300°C; *m* dead zone, 260°C; *n* central region, 260°C; *o* dead zone, 240°C; *p* central region, 240°C

15 Development of bainite in dead zone and central region of sample given longitudinal true strain of −0·63 (thermomechanical cycle shown in Fig. 3*c*) as function of isothermal hold temperature (OM)

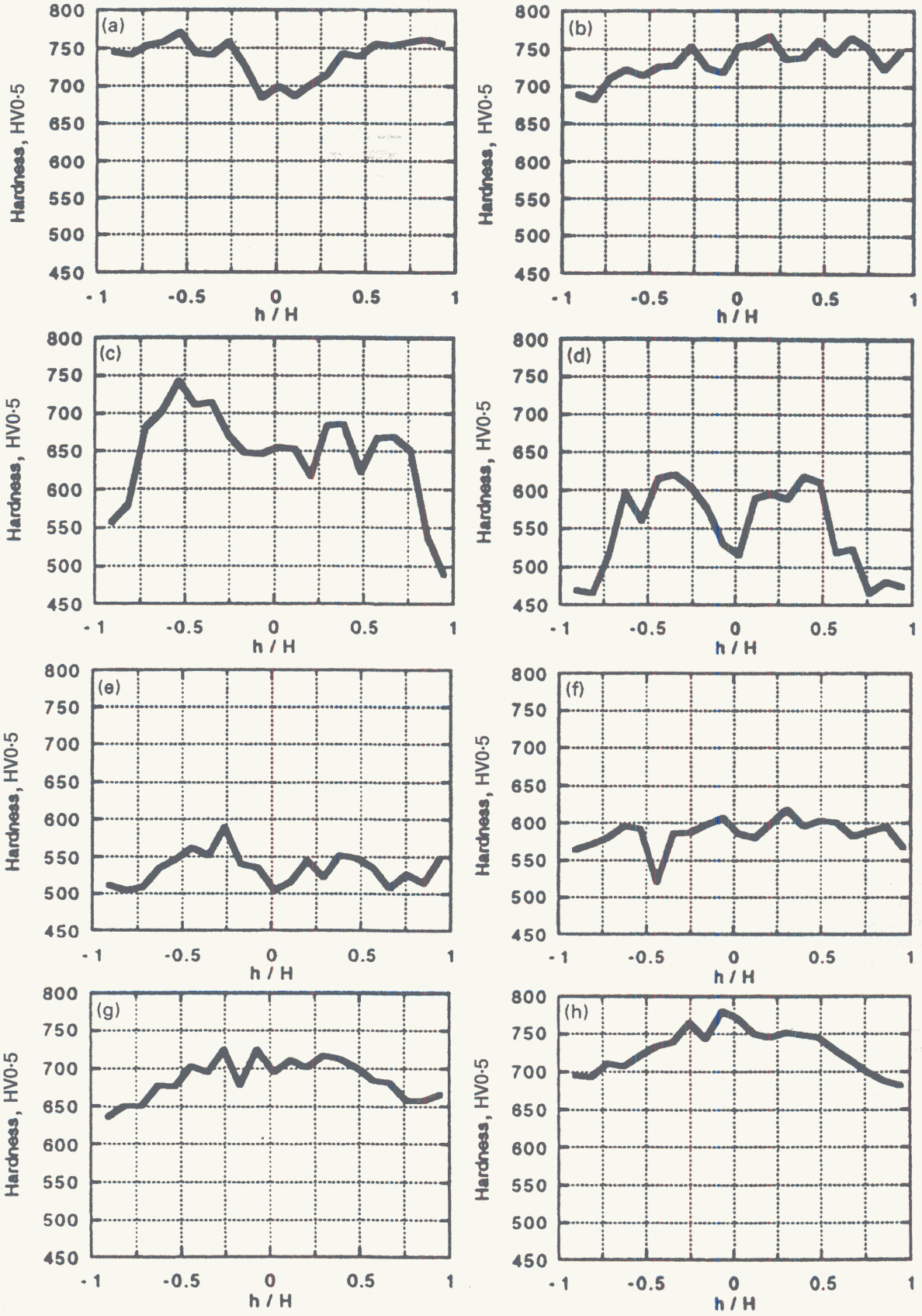

a 500°C; *b* 480°C; *c* 440°C; *d* 400°C; *e* 360°C; *f* 300°C; *g* 260°C; *h* 240°C

16 Hardness profiles along specimen axes of samples (following thermomechanical cycle shown in Fig. 3*c*) for various isothermal hold temperatures (*H* = cylinder half height, *h* = distance from centre of specimen)

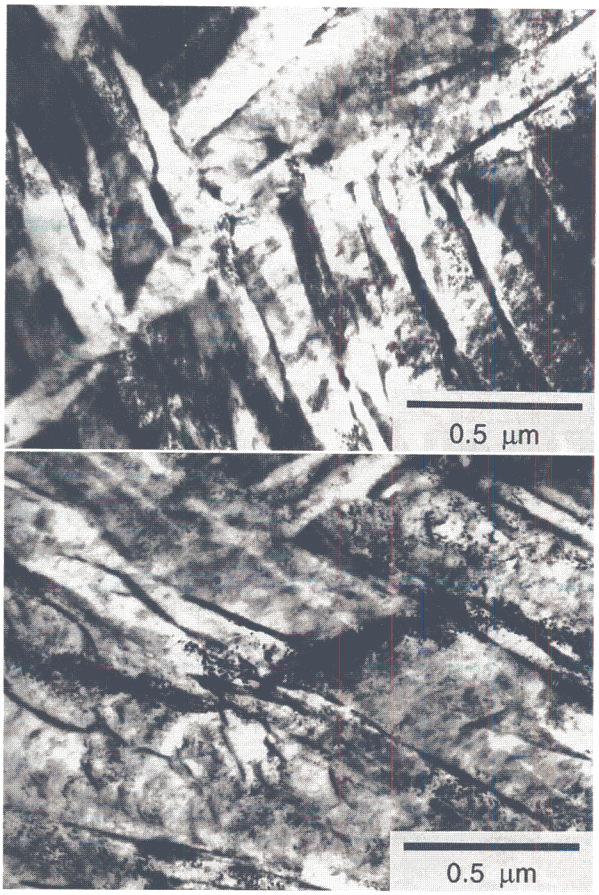

a dead zone; *b* deformed central region

17 TEM images of representative areas of sample deformed to longitudinal true strain of −0·63 and subsequently held at 260°C (thermomechanical cycle shown in Fig. 3*c*): white or lighter shaded areas are bainite, surrounded by darker martensite

platelet becomes more refined at low temperatures. The effect is present in both the deformed core and the dead zone region, indicating that the speed of bainite formation is generally retarded. The observations are consistent with the data presented in Table 1, where the hardness traverses a minimum with transformation temperature; however, the almost complete retardation of the bainite transformation at 240°C in the highly deformed core (Fig. 15*p*) is surprising and requires further investigation.

Conclusions

It has been demonstrated conclusively that the bainite transformation can be mechanically stabilised in a manner identical to the mechanical stabilisation of martensite in steels. The mechanism appears to be that the growth of bainite is retarded by the deformation debris in the austenite; heterogeneous nucleation becomes more frequent as defects are introduced into the austenite, but their growth by a displacive mechanism is stifled as the interface encounters forests of dislocations. Deformed austenite therefore transforms to a smaller quantity of bainite than undeformed austenite, and any bainite that forms is more refined. However, when the strain in the austenite is increased beyond a certain but undefined critical value, the enhanced nucleation compensates for the hindrance to growth, and the volume fraction of transformation achieved may be similar to that of undeformed austenite. The formation of pearlite is found to be accelerated by straining the austenite.

Acknowledgements

The authors are grateful to the Engineering and Physical Science Research Council and to the 'Atomic arrangements: design and control project' (a collaborative venture between the Research and Development Corporation of Japan and Cambridge University) for supporting the present work. The authors also thank Professor C. Humphreys for the provision of laboratory facilities at the University of Cambridge and Dr S. M. Roberts for assistance with finite element modelling.

References

1. E. S. MACHLIN and M. COHEN: *Trans. AIME*, 1951, **191**, 746–754.
2. H. C. FIEDLER, B. L. AVERBACH, and M. COHEN *Trans. ASM*, 1955 **46**, 267–290.
3. W. C. LESLIE and R. L. MILLER: *Trans. ASM Q.*, 1964, **57**, 972–979.
4. J. R. STRIFE, M. J. CARR, and G. S. ANSELL: *Metall. Trans.*, 1976, **8A**, 1471–1484.
5. V. RAGHAVAN: in 'Martensite, a tribute to Morris Cohen', (ed. G. B. Olson and W. S. Owen), 197–226; 1992, Materials Park, OH, ASM International.
6. K. TSUZAKI, S. FUKASAKU, Y. TOMOTA, and T. MAKI: *Mater. Trans. JIM*, 1991, **32**, 222–228.
7. J. R. PATEL and M. COHEN: *Acta Metall.*, 1953, **1**, 531–538.
8. J. W. CHRISTIAN: *Metall. Trans.*, 1982, **13A**, 509–538.
9. H. K. D. H. BHADESHIA: 'Bainite in steels', 1992, London, The Institute of Materials.
10. A. T. DAVENPORT: in 'The hot deformation of austenite', (ed. J. B. Ballance), 517–536; 1977, New York, TMS-AIME.
11. K. TSUZAKI, T. UEDA, K. FUJIWARA, and T. MAKI: in 'New materials and processes for the future', (ed. N. Igata *et al.*), 799–804; 1989, California, CA, SAMPE.
12. C. Y. HUANG, J. R. YANG, and S. C. WANG: *Mater. Trans. JIM*, 1993, **34**, 658–668.
13. Y. E. SMITH and C. A. SIEBERT: in 'Applications of modern metallographic techniques', STP 480, 131–151, 1970, Philadelphia, PA, ASTM.
14. Y. E. SMITH and C. A. SIEBERT: *Metall. Trans.*, 1971, **2**, 1711–1725.
15. T. MAKI: 'Physical metallurgy of direct-quenched steels', (ed. K. A. Taylor *et al.*), 3–16; 1993, Warrendale, PA, The Minerals, Metals and Materials Society.
16. R. H. EDWARDS and N. F. KENNON: *Metall. Trans.*, 1978, **9A**, 1801–1809.
17. R. FREIWILLIG, J. KUDRMAN, and P. CHRASKA: *Metall. Trans.*, 1976, **7A**, 1091–1097.
18. S. BHATTACHARYYA and G. L. KEHL: *Trans. ASM.*, 1955, **47**, 351–379.
19. A. MATSUZAKI, H. K. D. H. BHADESHIA, and H. HARADA: *Acta Metall. Mater.*, 1994, **42**, 1081–1090.
20. H. TAMEHIRO, M. MURATA, and R. HABU: in 'HSLA steels: metallurgy and applications', (ed. J. M. Gray *et al.*), 325; 1986, Metals Park, OH, ASM International.
21. P. H. SHIPWAY and H. K. D. H. BHADESHIA: *Mater. Sci. Eng. A*, 1995, **201**, 143–149.
22. H. K. D. H. BHADESHIA: in 'Recent advances in welding science and technology', (ed. S. A. David and J. M. Vitek), 189–198; 1989, Materials Park, OH, ASM International.